# DYNAMICS OF CHAIN EXCHANGE BETWEEN SELF-ASSEMBLED DIBLOCK COPOLYMER MICELLES OF POLY(ETHYLENE OXIDE)-*block*-POLYLACTIDE STUDIED BY DIRECT NONRADIATIVE EXCITATION ENERGY TRANSFER

Štěpán Popelka[a1], Luďka Machová[a2], František Rypáček[a3], Milena Špírková[a4], Miroslav Štěpánek[b1], Pavel Matějíček[b2] and Karel Procházka[b3,*]

[a] *Institute of Macromolecular Chemistry, Academy of Sciences of the Czech Republic, Heyrovského nám. 2, 162 06 Prague 6, Czech Republic; e-mail: [1] popelka@imc.cas.cz, [2] machova@imc.cas.cz, [3] ryp@imc.cas.cz, [4] spirkova@imc.cas.cz*

[b] *Department of Physical and Macromolecular Chemistry, Faculty of Science, Charles University, Albertov 6, 128 40 Prague 2, Czech Republic; e-mail: [1] stepanek@natur.cuni.cz, [2] matej@vivien.natur.cuni.cz, [3] prochaz@vivien.natur.cuni.cz*

Received June 3, 2005
Accepted August 1, 2005

*Dedicated to our great friend and colleague Dr. Marta Pacovská who left us for ever a year ago.*

A series of diblock poly(ethylene oxide)-*block*-polylactide copolymers with fairly narrow distribution of molar masses and compositions was prepared and characterized. The copolymers form multimolecular spherical micelles in 1,4-dioxane–water mixtures. The chain exchange between micelles formed by fluorescence-labeled copolymers was studied by direct nonradiative excitation energy transfer (NRET) fluorescence measurements in water-rich media containing 10 vol.% of 1,4-dioxane. The equilibration rate, i.e., the rate of unimer chain exchange between micelles obeys basically the theoretically predicted scaling relations. It slows down with the length of soluble blocks (a quadratic decrease) and considerably (an exponential decrease) with the length of insoluble chains. Scaling exponents were found lower than those predicted. The study shows that nanoparticle systems based on poly(ethylene oxide)-*block*-polylactide copolymers with required properties for various biomedical applications can be designed, prepared and their properties can be optimized.

**Keywords**: Block copolymers; Self assembly; Micelles; Biodegradable polymers; Light scattering; Fluorescence spectroscopy; Atomic force microscopy.

Biodegradable amphiphilic block copolymers are an attractive subject of study due to their potential applications in pharmacy and medicine. Special attention is paid to copolymers comprising poly(ethylene oxide) (PEO) as a hydrophilic block and a biodegradable aliphatic polyester, e.g., polylactide (PLA) as a hydrophobic block. Both constituents are biocompatible materials approved for clinical use by food and drug administration (FDA).

Poly(ethylene oxide), called also poly(ethylene glycol), has unique properties in water[1,2]. At room temperature PEO is completely miscible with water, regardless of the degree of polymerization. Its polymer chains are highly hydrated as a result of strong interactions, via hydrogen bonds with water molecules, and has a large excluded volume as evidenced by a high value of second virial coefficient[3]. In addition, the neutral linear chains without side groups show high mobility of polymer segments compared with other non-ionic water-soluble polymers. Above all, these properties of PEO may result in its low affinity to biomolecules such as proteins or other colloidal particles. Majority of PEO-derived pharmaceutical applications are based on this feature. The PEO-coated ("pegylated") peptides, proteinaceous drugs and polymer nanoparticles induce much lower immune response of the body and exhibit longer circulation times in blood, which both are related to lower interaction with plasma complements and, therefore, resulting in higher performance of these devices compared with their unmodified counterparts.

Polylactide together with polyglycolide and poly(6-caprolactone) belong to the group of aliphatic polyesters[4], which are the most widely used synthetic degradable polymers. The monomers, lactones, can be copolymerized by controlled polymerization and the properties of copolymers relevant to biomedical applications, such as degradability, mechanical properties or miscibility with drugs, can be tuned to a particular purpose by varying the composition and molecular weight. Typical applications of these biomaterials are surgical sutures, orthopedic devices and drug delivery systems[5]. More recently, they became studied as supporting materials for tissue regeneration[6–8].

Block copolymers of PEO and PLA combine the unique properties of both homopolymeric structures. They can be prepared by controlled polymerization of lactide initiated by OH end-groups of PEO as a co-initiator. As a catalyst, tin(II) 2-ethylhexanoate is most frequently used[9]. According to the telechelic type of PEO, containing either one or two OH end groups, diblock or triblock copolymers can be prepared, respectively. Due to biocompatibility and biodegradability, the potential of these copolymers for drug delivery formulations has been recognized in the eighties of the last century[10].

In aqueous solutions the copolymers form nanoparticles, with a hydrated poly(ethylene oxide) shell and a hydrophobic polylactide core[11–13], in which other hydrophobic compounds, such as drugs, can be incorporated. Therefore, the colloids prepared from PEO–PLA copolymers have been extensively studied as potential carriers for parenteral delivery of lipophilic

drugs[14–17], including paclitaxel[18], taxol[19] or adriamycin[20,21]. Typically, nano-assemblies of amphiphilic block copolymers are in a dynamic equilibrium with free copolymer molecules in solution (unimers). The unimer exchange rate is closely related to the rate of micelle disassembly, e.g. after dilution or change of composition of the solution. Micelle stability is an important factor for drug release kinetics and the lifetime of such a delivery system in vivo[22]. While the assemblies of water-soluble PEO–PLA copolymers with short PLA blocks exhibited poor circulation time after injection and dilution in blood[17], the particles formed from copolymers with a relatively high-molecular-weight hydrophobic block exhibited longer lifetime in blood circulation[23]. Although copolymers with prevailing hydrophobic blocks are usually insoluble in water, they can be made to form nanoparticles, using an intermediate solvent and a simple preparation procedures[23,24,16]. To optimize such a system, the information about the exchange rate of unimers between the particles formed by copolymers with different molecular parameters becomes of key importance. The present work was aimed at investigation of the unimer exchange between nanoparticles of PEO–PLA block copolymers and evaluation of the effect of the copolymer size and the ratio of hydrophobic and hydrophilic blocks on the unimer exchange rate. For this purpose, a series of PEO–PLA diblock copolymers, covering a wide range of molecular sizes and exhibiting different PLA/PEO ratios were synthesized and fluorescence-labeled. The chain exchange dynamics of the copolymers in aqueous systems was studied by nonradiative energy transfer method.

## EXPERIMENTAL

### Materials

*Chemicals.* Dichloromethane (DCM), dimethyl sulfoxide (DMSO), tetrahydrofuran (THF) and the other solvents used in the syntheses (Lachema Brno, Czech Republic) were purified by conventional methods[25]. 1,4-Dioxane of UV spectrophotometric grade (Fluka) was used for preparation of micellar solutions without further purification. Triethylene glycol monomethyl ether (TEGM) (Fluka) was twice distilled over $LiAlH_4$ under reduced pressure. Ethylene oxide (Fluka) was dried for 3 days over $CaH_2$ in a storage glass vessel equipped with a brass vent. DL-Lactide (Aldrich) was purified by recrystallization from a mixture of dry ethyl acetate and toluene (1:1). Tin(II) 2-ethylhexanoate (Aldrich), $Sn(Oct)_2$, was purified by double vacuum distillation. 9-(Chloromethyl)anthracene, dicyclohexylcarbodiimide (DCC), 4-(dimethylamino)pyridine (DMAP), (1-naphthyl)acetic acid, all from Fluka or Sigma, were used as received. Water was purified with a MilliQ Plus System (Millipore).

*Synthesis of (9-anthryl)acetic acid.* 9-(Chloromethyl)anthracene (2.5 g, 11 mmol) in dry DMSO (18 ml) was added dropwise to a solution of dry NaCN (0.89 g, 18 mmol) in DMSO (10 ml). The mixture was stirred at 35 °C and monitored by TLC (silica gel/chloroform–

petroleum ether, 1:1). After 4 h, the dark red mixture was diluted with 400 ml of water and the obtained yellow suspension was extracted with chloroform (3 × 30 ml). The water phase was saturated with NaCl and extracted again with chloroform (2 × 30 ml). The combined chloroform extracts were evaporated to dryness under reduced pressure. The solid residue was suspended together with 1 g (18.7 mmol) of KOH in a mixture of triethylene glycol (15 ml) and water (2 ml). The suspension dissolved to a dark red solution when heated. The solution was stirred at 100 °C for 10 h. After cooling, the mixture was diluted with 30 ml of water and neutralized with 2.5 M $H_2SO_4$. The precipitated yellow product was collected by filtration, washed with cold water and finally recrystallized three times from glacial acetic acid. Yield 0.23 g (12%), m.p. 224 °C. For $C_{16}H_{12}O_2$ (236.3) calculated: 81.34% C, 5.12% H; found: 81.0% C, 5.4% H. $^1$H NMR (acetone-$d_6$): 8.49 s, 1 H (H-arom.); 8.35 d, 2 H (H-arom.); 8.04 d, 2 H (H-arom.); 7.53 m, 4 H (H-arom.); 4.68 s, 2 H ($CH_2COOH$).

*Synthesis of block copolymers*. Polymerizations were prepared and performed under inert gas in sealed tubes equipped with a stirring bar. The copolymers used in this study were prepared in two steps. First α-methyl-ω-hydroxy-poly(oxyethylene) (mPEO) was prepared by anionic polymerization of ethylene oxide initiated with a mixture of triethylene glycol monomethyl ether and its potassium alcoholate as described in ref.[26] Typical procedure was as follows. Potassium metal (1 g, 26 mmol) was dissolved in TEGM (15.3 ml, 97 mmol) under reduced pressure. This solution of initiator (0.3 ml, 1.92 mmol) was dosed with a syringe into a graduated glass tube followed by monomer (48.95 g), which was transferred as gas from a storage vessel through a steel capillary and liquefied in the tube by cooling it in dry-ice/ethanol bath. The polymerization proceeded at 40 °C while stirring. After 3 days the tube content solidified. The crude polymer was dissolved in water, dialyzed and isolated by freeze-drying (yield 48.7 g, 99%). In this way, three samples of mPEO were prepared using different amounts of the initiator. The GPC-determined molecular weights $M_n$ and polydispersities ($M_w/M_n$) were as follows: 5600 (1.05), 15 100 (1.03) and 23 810 (1.04).

In the second step, the poly(DL-lactide) block was synthesized by controlled ring-opening polymerization of DL-lactide using mPEO with OH end-groups as a polymer co-initiator and tin(II) 2-ethylhexanoate as a catalyst. The monomer and co-initiator were dosed into a polymerization tube in the required ratio and dissolved in dry toluene under stirring and gentle heating. The catalyst was added in a dry toluene solution (0.12 mol/l) to achieve the catalyst/co-initiator mole ratio 2:1. The polymerization reached equilibrium conversion in 3 h at 85 °C. Then the copolymer was recovered by precipitation into twenty-fold excess of diethyl ether and dried in vacuum at 40 °C. Typical yields for copolymers were 96%. Molecular parameters were evaluated by GPC and $^1$H NMR.

*Labeling of block copolymers*. The prepared copolymers of mPEO–PDLLA were labeled at the free end of PDLLA block with a single naphthalene or anthracene derivative thus forming a pair for the Förster energy transfer. The labeling was performed by esterification of OH polymer end-groups with (1-naphthyl)acetic acid or (9-anthryl)acetic acid in the presence of dicyclohexylcarbodiimide (DCC)[27].

To label the amount of 300 mg of the copolymer containing 7–40 μmol of OH end-groups a solution of activated ester was prepared by mixing the DCM solutions of DCC (0.22 mmol, 0.54 mol/l), (1-naphthyl)acetic acid (0.18 mmol, 0.39 mol/l) and DMAP (0.004 mmol, 0.8 mol/l). The resulting mixture was filtered through an 0.5 μm PTFE syringe filter, added to the copolymer solution in 1.5 ml of DCM and the solution was stirred at room temperature for 10 h. After dilution with 5 ml of DCM, the fine precipitate of dicyclohexylurea was removed with a 0.5 μm PTFE syringe filter. The labeled copolymer was precip-

itated from the solution into diethyl ether, collected by filtration and dried in vacuum at 45 °C. Typical yield was 80–90%.

The same molar ratio and concentration of reagents was used for the labeling with (9-anthryl)acetic acid; however, THF was used as a solvent, because of low solubility of (9-anthryl)acetic acid in DCM. In this case mere precipitation was found insufficient to remove low-molecular-weight components from the reaction mixture. Hence, separation was performed by preparative GPC using a 2.5 × 50 cm column filled with Sephadex LH20 in THF, followed by UV detection. Collected polymer fractions were concentrated on a rotary evaporator, precipitated in diethyl ether and dried in vacuum at 45 °C. Typical yield was 70–85%.

*Solubility tests*. 3 mg of each copolymer sample was suspended in 1 ml of dioxane–water mixture. The suspension was vigorously shaken 5 h at 25 °C. The composition of the solvent was varied from 0 to 80 vol.% of dioxane.

*Preparation of micelles*. Block copolymer samples were dissolved overnight under stirring in a mixture of 1,4-dioxane with 20 vol.% of water. This mixture is a selective solvent for PEO and a mild selective precipitant for PLA. Therefore, spherical multimolecular reversible micelles form spontaneously upon dissolution. They coexist in equilibrium with a low fraction of unimers. In this mildly selective solvent, fairly fast exchange of unimers between micelles occurs. Then the water content was adjusted to 90 vol.% by a fast addition of water under stirring. The fast transfer into more selective solvent slows down the exchange kinetics considerably.

Consequently, it was found by the fluorescence-based monitoring of the exchange kinetics that in some cases (for samples with long insoluble PLA blocks) the system was quenched, i.e., the chain exchange kinetically frozen. In this case, the association number and size parameters do not presumably correspond to thermodynamic conditions of the water-rich solvent, but to those of the previous 1,4-dioxane-rich solvent. However, the micellization equilibrium of well-soluble samples with short PLA blocks readjusted to the conditions in the water-rich solvent. This is why we selected for detailed light scattering and fluorescence studies and for evaluation of scaling exponents only the well-soluble samples, the micellization of which is controlled by thermodynamic conditions existing in water-rich mixture with 10% of 1,4-dioxane, where the study has been performed.

## Methods

*$^1$H NMR spectroscopy*. The prepared polymers were analyzed by $^1$H NMR spectroscopy, using a Bruker Avance DPX-300 spectrometer operating at 300 MHz, with acetone-$d_6$ as solvent. Molecular weight of PDLLA block in $CH_3(OCH_2CH_2)_n$-$[OCOCH(CH_3)]_m$-OH was estimated from integrated areas of CH groups in lactide units (5.19 ppm), $CH_2$ groups in oxyethylene units (3.28 ppm) and the known molecular weight of mPEO block.

The content of anthracene and naphthalene moieties in labeled copolymers was determined from $^1$H NMR spectra on the basis of the peak intensity ratio of the aromatic protons (anthracene δ 8.5–7.5 ppm, naphthalene δ 8.0–7.4 ppm) of the label to the methylene protons ($OCH_2CH_2$) of the PEO block.

*Gel permeation chromatography*. GPC measurements were carried out on a modular system using coupled PLgel $10^3$ X, 10 :m (7.5 × 600 mm) and PLgel MIXED C, 5 :m (7.5 × 600 mm) columns with Waters 410 RI and Waters 484 detectors and THF as eluent. Molecular parameters were calculated using calibration with poly(ethylene oxide) standards.

*Steady-state fluorometry*. Steady-state fluorescence spectra (i.e., corrected excitation and emission spectra) were recorded with a SPEX Fluorolog 3 fluorimeter, USA, in a 1-cm quartz cuvette closed with a Teflon stopper.

*Light Scattering*. The light scattering setup (ALV, Langen, Germany), used for both static (SLS) and dynamic (DLS) measurements, consisted of a 633 nm He-Ne laser, an ALV CGS/8F goniometer, an ALV High QE APD detector and an ALV 5000/EPP multibit, multitau autocorrelator. The solutions for measurements were filtered through 0.45 μm Acrodisc filters. The measurements were carried out for different concentrations (0.1–3 mg/ml) and different angles at 20 °C. The measurements for the low ionic strength solutions were performed in quartz cells.

The SLS data were treated by the standard Zimm method using the equation

$$\frac{4\pi^2 n_0^2 (\mathrm{d}n/\mathrm{d}c)^2}{\lambda^4 N_\mathrm{A}} \frac{c}{R^{\mathrm{cor}}(q,c)} = \frac{1}{M_\mathrm{w}} \left(1 - \frac{1}{3} R_\mathrm{g}^2 q^2\right)^{-1} + 2A_2 c \qquad (1)$$

where $n_0$ is the refractive index of the solvent, ($\mathrm{d}n/\mathrm{d}c$) is the refractive index increment of the polymer with respect to the solvent, $\lambda$ is the wavelength of the incident light, $N_\mathrm{A}$ is the Avogadro constant, $R^{\mathrm{cor}}(q,c)$ is the corrected Rayleigh ratio, which depends on the polymer concentration $c$ and on the magnitude of the scattering vector, $q = (4\pi n_0/\lambda) \sin(\vartheta/2)$, where $\vartheta$ is scattering angle, $M_\mathrm{w}$ is the apparent weight-average molar mass of scattering polymeric particles, $A_2$ is the "light-scattering-weighted" second virial coefficient of the concentration expansion and $R_\mathrm{g}$ is the radius of gyration of scattering polymeric particles.

The refractive index increments, $\mathrm{d}n/\mathrm{d}c$, were measured on a Brice–Phoenix differential refractometer. For PLA–PEO micelles in 1,4-dioxane–water mixtures, the preferential sorption of solvent components in micelles plays an important role and increments at the osmotic equilibrium of the low-molar-mass components, $(\mathrm{d}n/\mathrm{d}c)_\mu$, have to be used. Increments were measured in a 50% 1,4-dioxane–water mixture, where the samples dissolve molecularly. They were recalculated to solvent mixtures differing in the content of 1,4-dioxane, taking into account the experimentally measured dependence of the refractive index of the 1,4-dioxane–water mixture.

DLS data analysis was performed by fitting the measured normalized intensity autocorrelation function $g_2(t) = 1 + \beta|g_1(t)|^2$, where $g_1(t)$ is the electric field correlation function, $t$ is the lag-time and $\beta$ is a factor accounting for deviation from the ideal correlation. An inverse Laplace transform of $g_1(t)$ with the aid of a constrained regularization algorithm (REPES)[28] provides the distribution of relaxation times, $\tau A(\tau)$

$$g_1(t) = \int_{-\infty}^{0} \tau A(\tau) \exp(-t/\tau) \, \mathrm{d} \ln \tau \, . \qquad (2)$$

Diffusion coefficients were calculated from mean times of individual diffusion modes, $\langle\tau\rangle$ as $D = 1/(\langle\tau\rangle q^2)$. Hydrodynamic radii, $R_\mathrm{H}$, were evaluated from the diffusion coefficients using the Stokes–Einstein formula. The viscosities and refractive indices of 1,4-dioxane–water mixtures (for the calculation of $R_\mathrm{H}$ values) were determined in previous studies[29].

*Atomic Force Microscopy*. All measurements were performed in the tapping mode under ambient conditions using a commercial scanning probe microscope, Digital Instruments NanoScope dimensions 3, equipped with a Nanosensors silicon cantilever, typical spring

constant 40 N/m. Polymeric micelles were deposited on a fresh (i.e., freshly peeled out) mica surface (flogopite, theoretical formula $KMg_3AlSi_3O_{10}(OH)_2$, Geological Collection of Charles University in Prague, Czech Republic) by a fast dip coating in a dilute micelle solution in dilute alkaline buffer (*c* ca. $10^{-2}$ g/l). After the evaporation of water, the samples for AFM were dried in a vacuum oven at ambient temperature for ca. 5 h.

## RESULTS AND DISCUSSION

### *Molecular Parameters of Prepared Copolymers*

Tables I and II summarize molecular parameters of α-methoxy-poly(ethylene oxide)-*block*-poly(DL-lactide) copolymers with a relatively wide range of molecular weights between 8000 and 45 000 the poly(DL-lactide) content in the range of 15–50 wt.% which were used to study the effect of copolymer composition on unimer exchange rate between copolymer micelles. The copolymers are referred as E(*n*)-L(*m*) where *n* and *m* represent number-average molecular weights $M_n$ of mPEO and PLA blocks in thousands, respectively.

### *Light Scattering*

Three relatively soluble samples (Table III) with approximately constant length of the insoluble PLA block ($M_{PLA}$ ca. 5000) and increasing length of the soluble PEO block ($M_{PEO}$ 5600–23 800) and two less soluble samples

TABLE I
Characteristics of block copolymers. $M_n$ was determined by GPC for the PEO block and by NMR for the PDLLA block. $M_w/M_n$ was determined by GPC

| Copolymer | $M_n$ (PEO) | $M_n$ (PDLLA) | $M_n$ (total) | $M_w/M_n$ | PLA, wt.% |
|---|---|---|---|---|---|
| E(6)-L(5) | 5600 | 4930 | 10530 | 1.11 | 47 |
| E(6)-L(3) | 5600 | 2570 | 8170 | 1.06 | 31 |
| E(6)-L(1) | 5600 | 1150 | 6750 | 1.04 | 17 |
| E(15)-L(14) | 15100 | 14400 | 29500 | 1.17 | 47 |
| E(15)-L(6) | 15100 | 5770 | 20870 | 1.19 | 28 |
| E(15)-L(2) | 15100 | 2370 | 17470 | 1.18 | 14 |
| E(24)-L(21) | 23800 | 21000 | 44800 | 1.20 | 47 |
| E(24)-L(10) | 23800 | 10060 | 33860 | 1.15 | 30 |
| E(24)-L(5) | 23800 | 4600 | 28400 | 1.14 | 16 |

TABLE II
Number of anthracene, $x_A$, and naphthalene, $x_N$, groups per PEO block of copolymer mPEO–PLA labeled by anthracene and naphthalene determined from $^1$H NMR spectra

| Copolymer | $x_A$ | Copolymer | $x_N$ |
|---|---|---|---|
| E(6)-L(5)-A | 0.95 | E(6)-L(5)-N | 0.97 |
| E(6)-L(3)-A | 0.29 | E(6)-L(3)-N | 1.19 |
| E(6)-L(1)-A | 0.30 | E(6)-L(1)-N | 0.93 |
| E(15)-L(14)-A | 1.27 | E(15)-L(14)-N | 0.95 |
| E(15)-L(6)-A | 1.13 | E(15)-L(6)-N | 1.21 |
| E(15)-L(2)-A | 1.32 | E(15)-L(2)-N | 1.23 |
| E(24)-L(21)-A | 1.49 | E(24)-L(21)-N | 1.38 |
| E(24)-L(10)-A | 0.94 | E(24)-L(10)-N | 1.11 |
| E(24)-L(5)-A | 1.29 | E(24)-L(5)-N | 1.25 |

TABLE III
Appearance of the mPEO–PLA copolymer/dioxane–water mixture after shaking at room temperature for 5 h (S, suspension; T, turbid solution; C, clear solution)

| Copolymer | Dioxane, vol.% | | | | | | |
|---|---|---|---|---|---|---|---|
| | 0 | 10 | 20 | 30 | 40 | 50 | 60 |
| E(6)-L(5) | S | T | T | C | C | C | C |
| E(6)-L(3) | S | C | C | C | C | C | C |
| E(6)-L(1) | C | C | C | C | C | C | C |
| E(15)-L(14) | S | S | S | T | T | C | C |
| E(15)-L(6) | S | T | C | C | C | C | C |
| E(15)-L(2) | C | C | C | C | C | C | C |
| E(24)-L(21) | S | S | S | S | S | T | C |
| E(24)-L(10) | S | S | S | T | C | C | C |
| E(24)-L(5) | S | S | C | C | C | C | C |

($M_{PLA}$ ca. 15 100 and 23 800, $M_{PEO}$ 14 400 and 10 000) were chosen for the study of the exchange rate from an extensive series of synthesized copolymers. The selected samples were characterized by static and dynamic light scattering. The values of refractive index increments were evaluated as described in the Experimental. The weight average molar masses obtained by the standard Zimm method are given in Table IV. The radii of gyration are too small and cannot be evaluated by static light scattering measurements. It is evident that the increasing length of soluble block results in a decrease in the aggregation number (for samples with the same length of insoluble block). The synthesized copolymers thus obey general theoretical predictions[30] confirmed experimentally for different micellizing systems[31] (see inset in Fig. 1). The size of micelles was characterized by dynamic light scattering. The distributions of hydrodynamic radii of micelles formed by co-

TABLE IV
Weight average molar masses, $(M_w)^{mic}$, aggregation numbers, $n_{agg} = (M_w)^{mic}/M_n$, and hydrodynamic radii, $R_H$, of mPEO–PLA micelles in dioxane–water mixture (10 vol.% dioxane)

| Copolymer | $(M_w)^{mic} \times 10^{-6}$, g/mol | $n_{agg}$ | $R_H$, nm |
|---|---|---|---|
| E(6)-L(5) | 1.65 | 157 | 11.7 |
| E(15)-L(6) | 1.83 | 88 | 16.7 |
| E(24)-L(5) | 1.91 | 67 | 18.8 |

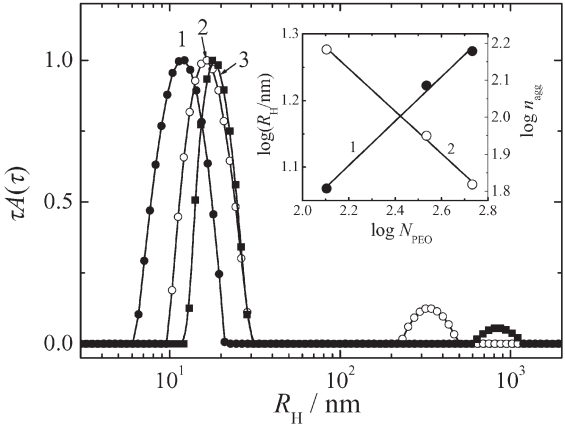


FIG. 1
DLS distributions of hydrodynamic radii of E(6)-L(5) (*1*), E(15)-L(6) (*2*) and E(24)-L(5) (*3*) micelles in 10% dioxane. Inset: hydrodynamic radii, $R_H$, and aggregation numbers, $n_{agg}$, vs number of PEO units for E(6)-L(5), E(15)-L(6) and E(24)-L(5) micelles

polymers with comparable length of insoluble blocks, $R_H$, measured at the scattering angle $\vartheta = 90°$, are plotted in Fig. 1, their hydrodynamic radii and aggregation numbers as functions of the length of soluble block, $M_{PEO}$, are shown in the inset. The distributions consist basically of one relatively narrow peak corresponding to micelles. Angular measurements show that the reciprocal relaxation time is proportional to $\sin^2 \vartheta$ (not shown). In some cases, traces of large particles were detected. They are most probably traces of dust particles present after filtration via 0.45 μm ultrafilters. It is necessary to take into account that the intensity of scattered light is proportional to the sixth power of size of particles and the recalculated number fraction falls deep below 1%.

The hydrodynamic radius, $R_H$, increases with increasing length of the soluble block, $M_{PEO}$, which is in agreement with theoretical predictions and observations of other authors[31]. The plot yields the empirical scaling exponent $\nu$ of about 0.3. Theoretically predicted values for the shell thickness of uncharged micelles, based on existing theories[30] and those observed experimentally[31] range from 0.5 to 0.7 according to solvent quality. The value obtained in this study is lower than literature values on similar systems. The discrepancy is due, in part to a non-negligible polydispersity of studied micelles. For a fully quantitative comparison, it is also necessary to keep in mind that the lengths of the insoluble blocks slightly differ in individual samples and that the association number and hence the size of micellar cores decreases as the shell thickness increases.

*Atomic Force Microscopy Characterization of Micelles*

Atomic force microscopy allows for visualization and measurement of sizes of nanoparticles deposited on the surface. Figure 2 shows a 3 × 3 μm tapping mode AFM scan of E(24)-L(5) micelles deposited on a mica surface by a

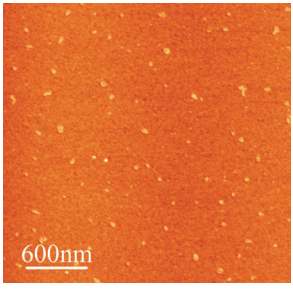


FIG. 2
The top view of a 3 μm × 3 μm AFM scan of E(24)-L(5) micelles deposited on mica surface

fast dip-coating from a dilute solution. The picture shows reasonably monodisperse, well-separated nanoparticles. The particles are pancake-deformed after deposition, but their dimensions (obtained by section analysis using the deconvolution technique correcting the finite size of the AFM tip) correspond roughly to those measured in solution. As it is evident from a low coverage of the surface, the micelles deposited from 1,4-dioxane–water solution do not stick properly to the mica surface and some of them may be rinsed off during the preparation of samples for imaging. It is the reason why we did not try to evaluate the polydispersity of micelles by AFM as we did in our earlier papers[32]. It is likely that larger micelles may adsorb at the surface more strongly than the small one and the AFM based distribution of sizes does not have to be a correct one.

*Fluorescence Study*

The main goal of the study was to measure the exchange rate of unimers between micelles. The exchange rate and the ability of reorientation of chains in nanoparticles are important factors that affect the behavior and stability of nanoparticles and have to be considered in the design, engineering and processing of successful biomedically applicable systems. In this work, we measured the overall rate of equilibration after mixing two otherwise identical micellar systems, which are labeled by two different fluorophores. Fluorescence measurements of nonradiative excitation energy transfer (NRET) have been often used for monitoring the exchange and equilibration rates in polymer systems[33–36].

The fluorophores (naphthalene or anthracene) were covalently attached at the ends of insoluble PLA blocks as described in the Experimental. Naphthalene (energy donor) and anthracene (energy acceptor) represent a suitable pair for NRET studies. The emission spectrum of naphthalene overlaps strongly with the absorption spectrum of anthracene, which is the prerequisite for an efficient NRET dipole–dipole interaction. Since the Förster radius, $R^0$, is fairly large (in nonviscous nonpolar solvents, ca. 2.1 nm [37]) and the PLA chains in the swollen core are close to each other and reasonably flexible and mobile, donors and acceptors may come close to each other in mixed cores. Hence the formation of mixed micelles should lead to a pronounced NRET effect. The normalized absorption and emission spectra of naphthalene-tagged copolymer, E(24)-L(5)-N (full lines *1* and *2*) and those of anthracene-tagged copolymer, E(24)-L(5)-A (broken lines *3* and *4*) are shown in Fig. 3 to demonstrate the strong spectral overlap. Spectra of other samples are identical and are not shown.

The overall rate of the chain exchange between micelles and formation of mixed micelles may be monitored by time-dependent energy transfer and characterized by its efficiency, $\chi(t) = \{1 - I_D(t)/I^0_D\}$, where $t$ is the time upon mixing, $I_D(t)$ is the time-dependent donor intensity at time $t$ after mixing and $I^0_D$ is the donor intensity in the absence of acceptor (one half of the intensity before mixing). The extent of mixing may be characterized by (i) the value $I_D(\infty)$, obtained for time approaching to infinity from the leveling off part of the curve, and (ii) by the ratio $I_D(\infty)/I^{fm}_D(\infty)$, where $I^{fm}_D(\infty)$ corresponds to the full (maximum) mixing and was obtained as follows: The "fully mixed micelles" were prepared by mixing individual micelles in a slightly selective 1,4-dioxane-rich solvent with 20% water, where a fast and easy exchange of unimers takes place. Mixed micelles were then quenched in a mixture of water with 10% of 1,4-dioxane (i.e., the water was added fast to slow down the exchange rate of unimers between micelles) and the donor intensity was measured.

The emission spectra were measured in the wavelength region from $\lambda$ = 300 to 500 nm (for excitation at 290 nm) at different times upon mixing and the rate of mixing was evaluated from the time dependence of the maximum intensity of the naphthalene band at $\lambda$ = 337 nm. The comparison of the emission spectrum obtained immediately after mixing the well-soluble samples E(24)-L(5)-N and E(24)-L(5)-A (in less than 1 min, curve *1*), excited at 290 nm with the theoretical average of spectra of pure

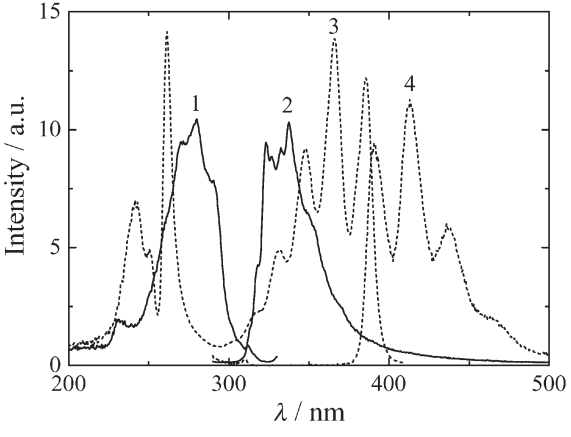


FIG. 3
Excitation and emission spectra of 1.5 g/l solution of E(24)-L(5)-N micelles (*1* excitation, *2* emission) and E(24)-L(5)-A micelles (*3* excitation, *4* emission) in 10% dioxane

samples before mixing (curve *2*) in Fig. 4 shows that an important initial intermixing proceeds on the time scale of seconds (less than 1 min). A relatively weak anthracene emission in the theoretical zero-time average spectrum is due to direct excitation of anthracene at $\lambda$ = 290 nm. This spectrum should be subtracted from all spectra measured at later times if anthracene emission were used for the evaluation of the time-dependent NRET efficiency. The observed non-negligible direct excitation of anthracene was one of reasons why we used only the changes in naphthalene emission in our study. It has been shown by several research groups that reliable evaluation of NRET should be based on the decrease in the donor (naphthalene) emission only, especially if the steady-state emission is measured[29,35,36]. In this case, the only complication may occur due to excimer formation, but the naphthalene excimers were not detected in this study[29]. As a typical example of spectral changes upon mixing, spectra for a mixture of E(24)-L(5)-N and E(24)-L(5)-A are shown in Fig. 5. The decrease in naphthalene emission and the concomitant increase in anthracene emission due to NRET are clearly evident. The dotted curve shows the spectrum of the fully mixed and equilibrated system, prepared in a slightly selective solvent 1,4-dioxane–20% water and quenched in a water-rich medium 1,4-dioxane–90% water. It is evident that even for the fastest equilibrating system, the NRET effect does not reach that observed in the corresponding "fully mixed micelles" prepared in a 1,4-dioxane-rich solvent and quenched in a water-rich solvent.

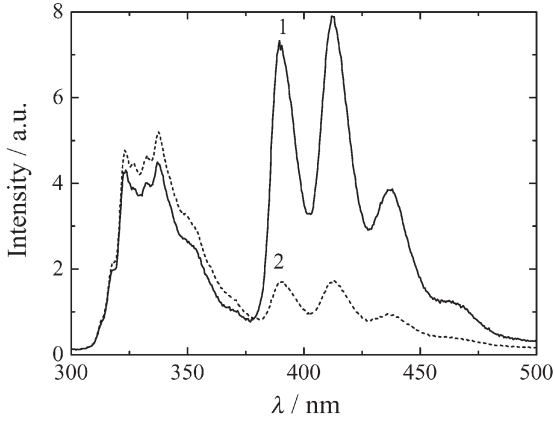


FIG. 4

Emission spectra (excitation 290 nm) of a mixture of E(24)-L(5)-N and E(24)-L(5)-A micelles (both 0.75 g/l) in 10% dioxane, immediately after mixing (*1*) and average of emission spectra (excitation 290 nm) of E(24)-L(5)-N and E(24)-L(5)-A micelles (concentration of both solutions 1.5 g/l) in 10% dioxane (*2*)

The energy transfer efficiency curves, $\chi(t) = \{1 - I_D(t)/I^0_D\}$ are shown in Fig. 6 for samples E(6)-L(5), E(15)-L(6), and E(24)-L(5) with almost the same lengths of insoluble PLA blocks (full curves) and for samples E(15)-L(14)

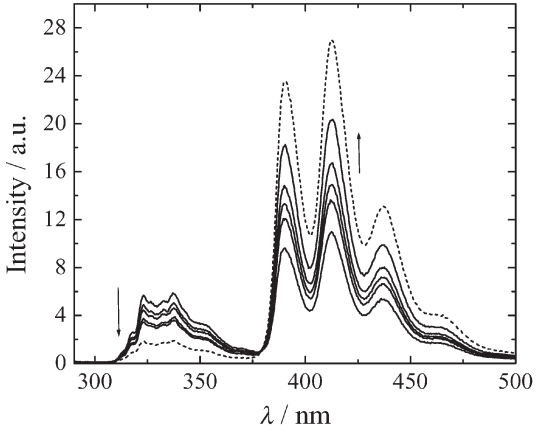


FIG. 5

Emission spectrum (excitation 290 nm) of a mixture of E(24)-L(5)-N and E(24)-L(5)-A micelles (both 0.75 g/l) in 10% dioxane, immediately and 20, 68, 240 and 1260 min after mixing. Arrows show the evolution of the spectrum with time. Dotted curve shows the emission spectrum (excitation 290 nm) of fully mixed micelles of E(24)-L(5)-N and E(24)-L(5)-A in 10% dioxane

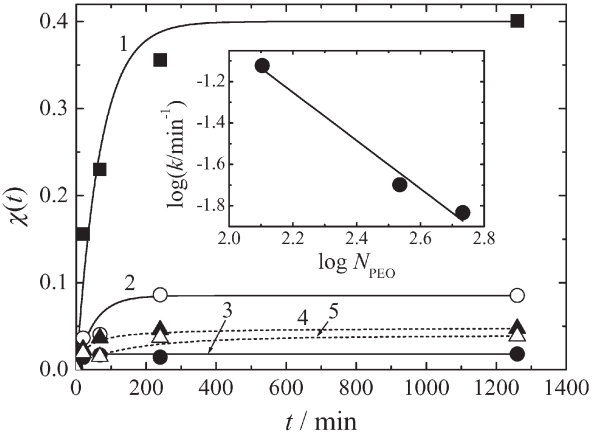


FIG. 6

Naphthalene-to-anthracene energy transfer efficiency, $\chi(t)$, measured in mixtures naphthalene- and anthracene-labeled micelles (both 0.75 g/l) of E(6)-L(5) (*1*), E(15)-L(6) (*2*), E(24)-L(5) (*3*), E(15)-L(14) (*4*) and E(24)-L(21) copolymers (*5*). Inset: rate constant, *k*, as a function of the number of PEO units, $N_{PEO}$

and E(24)-L(21) with fairly long PLA blocks (broken curves). The time dependence is non-exponential, which is in agreement with our earlier observations[29]. The process consists of a faster initial exchange of chains and a slower conformational equilibration, but the contribution of the fast process is prevailing. A fully quantitative treatment of NRET and evaluation of the rate of exchange of individual chains is complicated because, after mixing and at early times (practically until full equilibration), the system contains two different types of micelles: donor-rich and acceptor-rich ones, and NRET differs in both types of micelles. Common fluorescence measurements yield an integral (ensemble average) response of the whole system. Nevertheless, the rate of NRET is proportional to the rate of the decisive equilibration processes, in this case, to the chain exchange rate. Moreover, for a potential use of micelles in targeted drug delivery systems and for studies of their dynamic behavior and long-time stability, the knowledge of the overall rate is usually sufficient.

The measured rate depends strongly on the length of the soluble block, i.e., it decreases with increasing length of the soluble block. At long times the curves level off but, as already mentioned, they do not reach the value measured for micelles prepared by the mixing in 1,4-dioxane-rich solvent. Hence the mixing is always (i.e., at times ca. $10^3$ min) incomplete, even though the curves clearly level off, and NRET is reduced, probably due to steric reasons. The energy-transfer-efficiency curves for two less soluble samples E(15)-L(14) and E(24)-L(21) with long PLA blocks are depicted by dotted curves. It is evident that the mixing is very slow for sample with $M_{PLA}$ ca. 15 000 and that the unimer exchange rate is even slower for micelles formed by copolymer with the $M_{PLA}$ ca. 24 000.

As mentioned above, the measured rate of donor fluorescence quenching caused by energy transfer is a result of a fairly complex integral response of the system and we realize that its comparison with theoretical predictions of the effect of copolymer structure on the rate of chain exchange processes between micelles is not straightforward. Nevertheless, we assume that the leading mechanism is the exchange of individual chains, i.e., the insertion/expulsion mechanism. This process is the slowest, i.e., the rate-determining step of the equilibration, since it assumes an energetically demanding hindered transport of insoluble PLA blocks through fairly concentrated shell formed by incompatible water-soluble PEO blocks. Therefore it is interesting to compare the experimentally measured rates with scaling laws proposed theoretically by Dormidontova[38]. The theory predicts the following dependences for the rate constants of the equilibrium exchange rate of chains on the lengths of individual blocks

$$k_{in} \propto \exp(n_{eq}^{1/2})/\tau_{un} \quad (3)$$

$$k_{ex} \propto \exp(n_{eq}^{5/6})/\tau_{un} \quad (4)$$

where $n_{eq}$ is the association number that does not depend, in the first approximation, on the length of soluble blocks and the characteristic time, $\tau_{un}$, necessary to reach the "activated escape state" scales $\tau_{un} \propto (N_{PEO})^{9/5}$. The association number depends on the length of insoluble blocks, $n_{eq} \propto (N_{PLA})^{4/5}$. According to theory, the exchange rate slows appreciably with increasing length of the soluble block (almost quadratic decrease has been predicted) and much more with the length of insoluble block (in principle, exponentially) because the slowest rate-determining "diffusion-like" penetration of the insoluble block through a fairly dense brush formed by incompatible blocks is more difficult and takes longer. In our study, we were reasonably able to test the dependence on the length of soluble PEO blocks only. A logarithmic plot of the NRET rate constant $k$ (obtained by a reasonably accurate single-exponential fitting) of mixing curves as $\chi(t) = a(1 - e^{-kt})$ vs log $N_{PEO}$ is shown in the insert of Fig. 6. The plot is linear and yields the scaling exponent ca. 1.2, i.e., 6/5. This is a lower value than that predicted, influenced by several factors: we monitor a fairly complex response of the system, the core-forming chains slightly differ in length, the "effective flexibility" of shell-forming PEO blocks increases with their length and the theory of Dormidontova is strongly simplified. We believe that the simplification in the theory may lead to slightly incorrect (higher) values of the scaling exponent. The theory assumes that the equilibrium association number does not depend on the length of the soluble block. More detailed theories, as well as a number of experimental studies (including this one – see Fig. 1) show that the association number decreases with increasing length of soluble blocks[30]. The core slightly shrinks with decreasing association number, but the number and density of chains in the shell decreases. The effects of decreasing density and increasing thickness partially compensate and do not hinder the penetration of PLA blocks through the shell formed by long PEO blocks so much as the simplified theory predicts.

## CONCLUSIONS

Poly(ethylene oxide)-*block*-polylactide copolymers with comparable lengths of both blocks (length ratio 1:1–4:1) form spherical core-shell micelles in 1,4-dioxane–water mixtures and in aqueous media. The self-assembly basi-

cally obeys the theoretically predicted scaling laws, even though a certain polydispersity of micelles formed by fairly short copolymers studied in this paper lowers the experimental values of scaling exponents.

The exchange rate of individual chains between micelles depends strongly on the lengths of both blocks. It decreases slightly with increasing length of the soluble PEO block and strongly with increasing length of the insoluble PLA block as predicted by the scaling theory.

Even though the NRET measurement yields a complex integral response of the system, the obtained rate constants reasonably scale with the length of the soluble block as predicted by theory.

In the water-rich 1,4-dioxane–90% water mixture, the rate of mixing slows down by one order of magnitude for molar masses of the soluble block increasing four times. Thus relatively small biocompatible self-assembled nanoparticle systems based on PLA–PEO can be designed and successfully manufactured.

Since the exchange rate slows down at least by one order of magnitude when going from the 1,4-dioxane–10% water mixture to pure water, the behavior and properties appropriate for potential applications in the field of targeted drug delivery together with sufficient kinetic stability of PLA–PEO self-assembled nanoparticles are guaranteed. They may be further optimized by selecting proper lengths of blocks.

*Š. Popelka, L. Machová, F. Rypáček and M. Špírková would like to acknowledge the financial support of the Grant Agency of the Academy of Sciences of the Czech Republic (Grants No. A4050202 and A400500505). M. Štěpánek, P. Matějíček and K. Procházka would like to acknowledge the support of the Grant Agency of the Czech Republic (Grants No. 203/02/D048 and No. 2003/04/0490) and the Marie Curie Training Network POLYAMPHI.*

**REFERENCES**

1. Lee J. H., Lee H. B., Andrade J. D.: *Prog. Polym. Sci.* **1995**, *20*, 1043.
2. Harris J. M., Zalipsky S.: *ACS Symp. Ser.* **1997**, 680.
3. Venohr H., Fraaije V., Strunk H., Borchard W.: *Eur. Polym. J.* **1998**, *34*, 723.
4. Ikada Y., Tsuji H.: *Macromol. Rapid Commun.* **2000**, *21*, 117.
5. Chasin M., Langer R.: *Biodegradable Polymers as Drug Delivery Systems*. Marcel Dekker, New York 2000.
6. Hutmacher D. W.: *Biomaterials* **2000**, *21*, 2529.
7. Hutmacher D. W.: *J. Biomater. Sci. Polym. Ed.* **2001**, *12*, 107.
8. Vozzi G., Flaim C. J., Bianchi F., Ahluwalia A., Bhatia S.: *Mater. Sci. Eng., C* **2002**, *20*, 43.
9. Albertsson A. C., Varma I. K.: *Biomacromolecules* **2003**, *4*, 1466.
10. Churchill J. R., Hutchinson F. G.: Eur. EP0166596A2 (1986).

11. Tanodekaew S., Pannu R., Heatley F., Attwood D., Booth C.: *Macromol. Chem. Phys.* **1997**, *198*, 927.
12. Heald C. R., Stolnik S., Kujawinski K. S., De Matteis C., Garnett M. C., Illum L., Davis S. S., Purkiss S. C., Barlow R. J., Gellert P. R.: *Langmuir* **2002**, *18*, 3669.
13. Riley T., Heald C. R., Stolnik S., Garnett M. C., Illum L., Davis S. S., King S. M., Heenan R. K., Purkiss S. C., Barlow R. J., Gellert P. R., Washington C.: *Langmuir* **2003**, *19*, 8428.
14. Lee J. Y., Cho E. C., Cho K.: *J. Controlled Release* **2004**, *94*, 323.
15. Gref R., Minamitake Y., Peracchia M. T., Trubetskoy V., Torchilin V., Langer R.: *Science* **1994**, *263*, 1600.
16. Riley T., Stolnik S., Heald C. R., Xiong C. D., Garnett M. C., Illum L., Davis S. S., Purkiss S. C., Barlow R. J., Gellert P. R.: *Langmuir* **2001**, *17*, 3168.
17. Hagan S. A., Coombes A. G. A., Garnett M. C., Dunn S. E., Davis M. C., Illum L., Davis S. S., Harding S. E., Purkiss S., Gellert P. R.: *Langmuir* **1996**, *12*, 2153.
18. Burt H. M., Zhang X., Toleikis P., Embree L., Hunter W. L.: *Colloid. Surf., B* **1999**, *16*, 161.
19. Zhang X. C., Jackson J. K., Burt H. M.: *Int. J. Pharm.* **1996**, *132*, 195.
20. Kataoka K., Kwon G. S., Yokoyama M., Okano T., Sakurai S.: *J. Controlled Release* **1993**, *24*, 119.
21. Piskin E., Kaitian X., Denkbas E. B., Kucukyavuz Z.: *J. Biomater. Sci., Polym. Ed.* **1995**, *7*, 359.
22. Allen C., Maysinger D., Eisenberg A.: *Colloid. Surf., B* **1999**, *16*, 3.
23. Gref R., Domb A., Quellec P., Blunk T., Muller R. H., Verbavatz J. M., Langer R.: *Adv. Drug Delivery Rev.* **1995**, *16*, 215.
24. Verrecchia T., Spenlehauer G., Bazile D. V., Murry-Brelier A., Archimbaud Y., Veillard M.: *J. Controlled Release* **1995**, *36*, 49.
25. Armarego W. L. F., Perrin D. D.: *Purification of Laboratory Chemicals*, 4th ed. Butterworth Heinemann, Bath 2000.
26. Kazanskii K. S., Lapienis G., Kuznetsova V. I., Pakhomova L. K., Evreinov V. V., Penczek S.: *Polym. Sci., Ser. A* **2000**, *42*, 585.
27. Hassner A., Alexanian V.: *Tetrahedron Lett.* **1978**, *46*, 4475.
28. Jakeš J.: *Czech. J. Phys. B* **1988**, *38*, 1305.
29. Matějíček P., Uhlík F., Limpouchová Z., Procházka K., Tuzar Z., Webber S. E.: *Macromolecules* **2002**, *35*, 9487.
30. Whitmore M. D., Noolandi J.: *Macromolecules* **1985**, *18*, 657.
31. Xu R., Winnik M. A., Riess G., Chu B., Croucher M. D.: *Macromolecules* **1992**, *65*, 644.
32. Matějíček P., Humpolíčková J., Procházka K., Tuzar Z., Špírková M., Hof M., Webber S. E.: *J. Phys. Chem. B* **2003**, *107*, 8232.
33. Procházka K., Bednář B., Mukhtar E., Svoboda P., Trněná J., Almgren M.: *J. Phys. Chem.* **1991**, *95*, 4563.
34. Wang Y., Kausch C. M., Moonseok C., Quirk R. P., Mattice W. L.: *Macromolecules* **1995**, *28*, 904.
35. Li M., Liu L., Jiang M.: *Macromol. Rapid Commun.* **1995**, *16*, 831.
36. Clements J. H., Webber S. E.: *J. Phys. Chem. B* **1999**, *103*, 9366.
37. Förster T.: *Discuss. Faraday Soc.* **1959**, *7*, 27.
38. Dormidontova E. E.: *Macromolecules* **1999**, *32*, 7630.